

## Research Article

## Open Access

Manawwer Alam\*, Naser M Alandis, Naushad Ahmad, Mohammad Asif Alam, Eram Sharmin

# Jatropha seed oil derived poly(esteramide-urethane)/ fumed silica nanocomposite coatings for corrosion protection

<https://doi.org/10.1515/chem-2019-0022>

received September 9, 2018; accepted December 17, 2018.

**Abstract:** Jatropha oil [JO] based poly (esteramide-urethane) coatings embedded with fumed silica nanoparticles were prepared. JO was converted to N,N-bis(2-hydroxy ethyl) JO fatty amide (HEJA) and was further modified by a tetrafunctional carboxylic acid (*trans* 1,2 diaminocyclo-hexane-N,N,N',N',-tetraacetic acid) to form poly (diamino cyclohexane esteramide) (PDCEA). PDCEA was then treated with toluene 2,4-diisocyanate and fumed silica to prepare poly(diamino cyclohexane urethane esteramide) (PUDCEA) nanocomposite. The formation of PDCEA and PUDCEA nanocomposites was confirmed by FTIR, <sup>1</sup>H & <sup>13</sup>C NMR spectroscopic techniques. The thermal behavior and morphology of PUDCEA nanocomposite coatings were investigated by TGA/DTG, DSC, SEM, EDX spectroscopy. PUDCEA nanocomposites were applied on carbon steel and their coatings were produced at room temperature. The properties of these nanocomposite coatings were investigated by standard analytical methods. The PUDCEA-3 nanocomposite showed good anticorrosion and physico-mechanical performance. These naocomposite coatings can be employed safely upto 200°C.

**Keywords:** Jatropha oil; *trans* 1,2diaminocyclo-hexane-N,N,N',N',-tetraacetic acid; poly(urethane esteramide); coatings.

\*Corresponding author: **Manawwer Alam**, Department of Chemistry, College of Science, King Saud University, P.O. Box 2455, Riyadh 11451, Saudi Arabia, E-mail: malamiitd@gmail.com; maalam@ksu.edu.sa

**Naser M Alandis, Naushad Ahmad:** Department of Chemistry, College of Science, King Saud University, P.O. Box 2455, Riyadh 11451, Saudi Arabia

**Mohammad Asif Alam:** Center of Excellence for Research in Engineering Materials(CEREM), King Saud University, P. O. Box 800, Riyadh 11421, Saudi Arabia

**Eram Sharmin:** Department of Pharmaceutical Chemistry, College of Pharmacy, Umm Al-Qura University, P.O. Box 715, Makkah Al-Mukarramah 21955, Saudi Arabia

## 1 Introduction

Industrial chemicals are mainly being obtained from fossil-based materials. The latter are not only costly and hazardous for human health and environment, but are also becoming less available, with time. Vegetable oils bear great potential attributes to provide alternative sustainable and eco-friendly equivalent substitutes to fossil-based materials [1-4]. Vegetable oils have as their main components triglycerides, which may be modified by different moieties such as diethanolamine, carboxylic acid, alcohol, styrene, and others. They may be utilized in the production of various polymeric materials such as polyesteramide, polyepoxy, polyurethane, polyetherimide, and their composites with other polymers [5-9]. Vegetable seed oils from linseed, castor, pongamia glabra, rapeseed, jatropha, soybean, and others are used for the synthesis of various polymers [10-13]. JO contains mostly oleic, linoleic, palmitic, and stearic acid. JO is also used for the preparation of polyesteramide, polyetheramide and other polymeric materials [14,15].

*trans* 1,2diaminocyclo-hexane-N,N,N',N',-tetraacetic acid(CDTA) is a tetrafunctional carboxylic acid. It is mainly applied as a ligand for transition metals, including zirconium, copper, nickel, and others, to form coordination complexes/compounds in field of coordination chemistry and as an anion exchanger for separation of rare earth element complexes [16-18].CDTA is also used for the electrochemical study of chromium complexes [19].

There are a large number of nanofillers like carbon nanotubes (CNT), multiwalled carbon nanotubes (MWNT), nanoclay, and nanoparticles, being used to reinforce polymer matrices, drastically improving polymer properties for many commercial applications [20,21]. Recently, polymeric resins modified with different nano metal oxides such as ferrite, Al<sub>2</sub>O<sub>3</sub>, CaO, SiO<sub>2</sub>, TiO<sub>2</sub>, CeO<sub>2</sub>, and ZnO, with improved physico-mechanical properties have been reported in the literature [22-25,29-31]. Nanoparticle inclusion in polymer resins have improved scratch hardness, tensile strength, thermal stability,

toughness, stiffness and can shift the glass transition temperature of polymeric resins [26]. Silica nanoparticles are widely used as inorganic fillers due to their controlled size, large surface area, uniform structure, and remarkable moisture-barrier properties. The preparation of silica-reinforced polymeric films for coating applications is of great interest. The silica nanoparticle reinforced polymeric films find variety of applications as coating materials [24]. In composite (hybrid) materials, due to physical and chemical interactions between molecules, the properties of composites are significantly affected in the vicinity of individual materials. The properties of nanocomposites are related to degree of thermosets, crystallinity, mobility chain confirmation, and interface with the matrix [27,28].

Polyurethanes (PUs) are elastic polymers used as elastomers and composites. PUs possesses unique properties and is used in various applications including foams, insulations, adhesives, sealants, coatings, and elastomers. For the preparation of urethane linkages through hydroxyl and isocyanate functions, various molecules are used, such as toluene diisocyanate(TDI), isophorone di isocyanate(3-isocyanatomethyl 3,5,5 tri methyl cyclohexylisocyanate) (IPDI), methylene bis(cyclohexylisocyanate)(HMDI), and others. However, it was found that: (i) IPDI was found to be less reactive than TDI, (ii) a greater amount of HMDI must be used compared to TDI, and (iii) HMDI resins enhance pot life and minimize defects [3, 34, 35].

The manuscript aims to present the synthesis of poly(diamino cyclohexane urethane esteramide) (PUDCEA) and investigate the effect of fumed silica on coating properties. The results of physico-mechanical and corrosion resistance performance show that PUDCEA nanocomposite coatings have desirable properties on mild steel substrate. Furthermore, this study of using JO for poly(diamino cyclohexane urethane esteramide) synthesis illustrates utilization of a sustainable resource that has not been reported earlier.

## 2 Experimental

### 2.1 Materials

Jatropha oil [14,15]; *trans*1,2 diamino cyclo-hexane-N,N',N',-tetraacetic acid(CDTA)(Sigma Chemicals, USA); toluene 2,4-diisocyanate(TDI)(Acros Organic, USA); sodium metal, methanol, xylene, diethanolamine, diethyl ether, and sodium chloride (BDH Chemicals, Ltd. Poole,

England); and fumed silica(surface area  $395\pm 25\text{m}^2/\text{gm}$ , size  $0.007\ \mu\text{m}$ , refractive index 1.46.) (Sigma Aldrich, USA).

### 2.2 Instruments and methods

FTIR spectra of PDCEA and PUDCEA nanocomposites were collected on an FTIR spectrophotometer (Spectrum 100, Perkin Elmer Cetus Instrument, Norwalk, CT, USA) using a KBr cell. NMR spectra ( $^1\text{H}$  and  $^{13}\text{C}$ ) were taken on a Jeol DPX400MHz (Japan), where deuterated chloroform and tetramethylsilane were used as solvent and internal standard, respectively. Thermal stability of PUDCEA nanocomposites was measured by TGA and DSC (Mettler Toledo AG, Analytical CH-8603, Schwerzenbach, Switzerland). Here nitrogen atmosphere was maintained and  $10^\circ\text{C}/\text{min}$  was the heating rate. The molecular weight of PUDCEA was investigated by gel permeation chromatography (GPC) (HT-GPC Module 350A, Viscotek, Houston, TX, USA) using tetrahydrofuran (THF) as eluent at a flow rate of  $1.0\text{mL}/\text{min}$ . The morphology of PUDCEA coatings was studied by scanning electron microscopy (SEM) (JEOL, JED-2200 Series, Japan). The topography of PUDCEA-coated panel was studied by atomic force microscopy (AFM) (A.P.E. Research, Basovizza 34149, Trieste, Italy). Physico-chemical studies of PDCEA and PUDCEA were evaluated by acid and hydroxyl value determination (ASTM D555-61 and ASTM D1957-86, respectively). Coating properties of PUDCEA were evaluated by refractive index (ASTM D1218), scratch hardness (BS 3900), adhesion crosshatch (ASTM D3359-02), impact test (IS 101 part 5  $\text{s}^{-1}$ , 1988), pencil hardness test (ASTM D3363-05), flexibility/bending test (ASTM D3281-84), gloss (by Glossmeter, Model: KSJ MG6-F1, KSJ Photoelectrical Instruments Co., Ltd. Quanzhou, China), and thickness (ASTM D 1186-B). The potentiodynamic studies of PUDCEA nanocomposite coatings were conducted with a Gill AC (ACM Instruments, Cumbria, UK). The potentiodynamic measurements of PUDCEA coatings were performed in a three-electrode system at ambient temperature in various corrosive environments (tap water, 3.5wt% NaCl, and 3.5wt% HCl), with a platinum electrode as the counter electrode and a saturated calomel electrode as the reference electrode. PUDCEA-coated mild steel specimen was used as the working electrode; the exposed surface area of  $1.0\ \text{cm}^2$  was fixed by a PortHoles electrochemical sample mask. Potentiodynamic polarization (PDP) was obtained using a sweep rate of  $1.0\ \text{mV}/\text{s}$  in the potential range  $\pm 250\ \text{mV}$  with respect to the open circuit potential. PDP was used to evaluate the corrosion protective

performance of PUDCEA coatings. Each coating system was evaluated in triplicate for corrosion protection.

### 2.3 Preparation of N,N-bis(2-hydroxy ethyl) JO fatty amide (HEJA)

The synthesis of HEJA was carried out as per a previously published paper [14, 15].

### 2.4 Synthesis of poly(diamino cyclohexane esteramide)(PDCEA)

Initially, 4.0 mol of HEJA were heated to 80°C, and 2.0 mol of CDTA were added in a four-neck round-bottomed flask, placed on a magnetic stirrer with a hot plate. This flask was fitted with a Dean Stark Trap, thermometer and nitrogen inlet tube. The reactants were heated to 200°C, and a small amount of xylene was added for azeotropic distillation. The acid value was determined at regular intervals of time to monitor the progress of the reaction.

After the desired acid value was achieved, the xylene solution of PDCEA was poured in a separating funnel and distilled water was added. The contents were swirled and were allowed to stand till the xylene and water layer separated. The water layer was removed and tested for unreacted acid. The washing process was repeated until the solution was free from any unreacted acid. The xylene solution was then passed through anhydrous sodium sulphate to remove traces of moisture followed by the removal of xylene in rotary evaporator. The pure PDCEA thus obtained was tested by FTIR and NMR.

### 2.5 Synthesis of poly(diamino cyclohexane urethane esteramide)(PUDCEA)

For urethane modification, 10 g PDCEA, dissolved in xylene (20mL), and TDI (10wt%, 12wt%,14wt%) were added in a four-neck round-bottomed flask, placed on a magnetic stirrer with a hot plate. This flask was fitted with a cold water condenser, Dean Stark Trap, thermometer and nitrogen inlet tube. The contents were heated to a temperature of 120°C. The progress of the reaction was monitored by the hydroxyl value. The solvent was evaporated by vacuum.

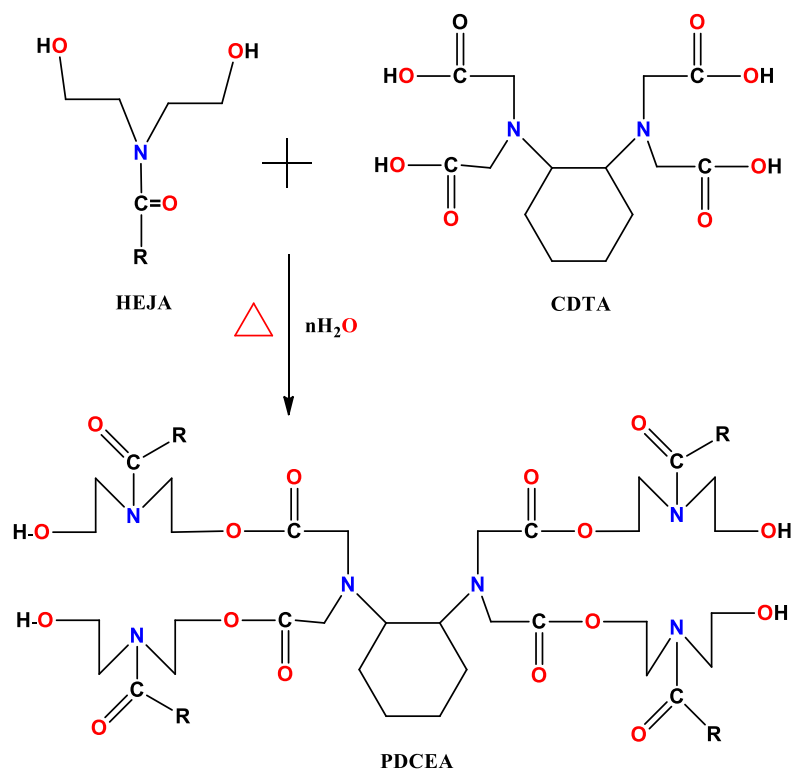
### 2.6 Synthesis of fumed silica modified poly(diamino cyclohexane urethane esteramide) (PUDCEA)

For nanocomposite preparation, PUDCEA, prepared from 12% TDI, was loaded with 1wt%, 2wt%, and 3wt% fumed silica before the urethane reaction. 10 g PDCEA was dissolved in xylene (20mL), and fumed silica was added in different percentages (1wt%, 2wt%, and 3wt%) at 30°C (to obtain PUDCEA-1, PUDCEA-2, PUDCEA-3, respectively). The contents of the flask were stirred for 30 minutes and then TDI (12 wt%) was added drop-wise to the reaction flask containing PDCEA and fumed silica. This flask was fitted with a cold water condenser, Dean Stark Trap, thermometer and nitrogen inlet tube. The contents were heated to a temperature of 120°C. The progress of the reaction was monitored by hydroxyl value determination at regular intervals of time. The solvent was evaporated by vacuum during the physico-mechanical testing; it was found that the 3wt% fumed silica in PUDCEA nanocomposite showed the best coating properties. PUDCEA-3 resin was dissolved in a 40% solution of xylene and applied by brush technique to mild steel panels. The coated panels are left to dry at room temperature After 10 days, coating became dry –to- hard; at this stage they were subjected to physico-mechanical and corrosion tests.

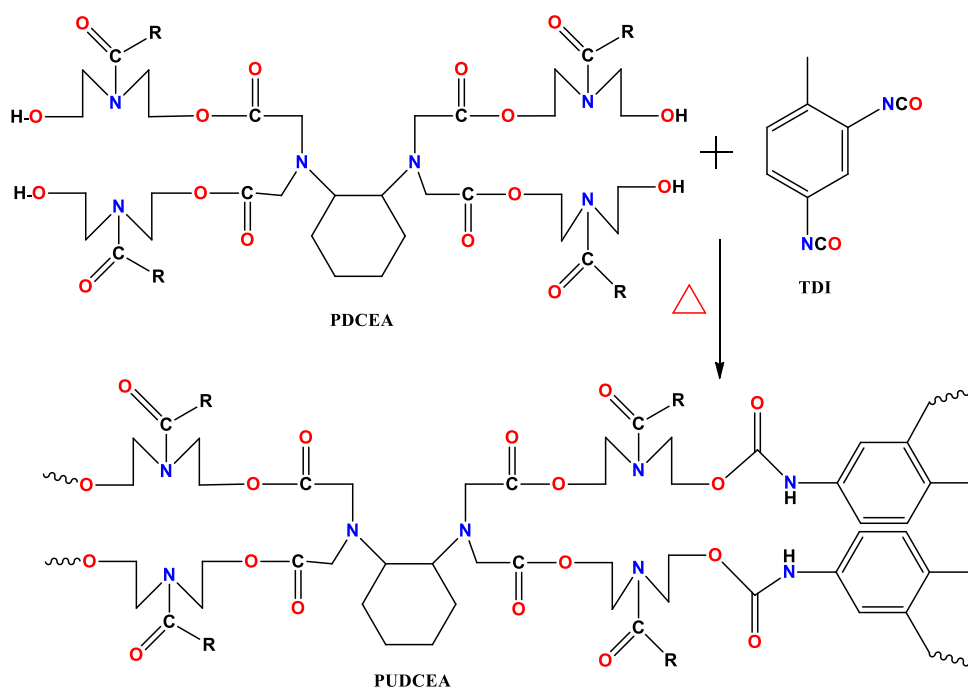
Ethical approval: The conducted research is not related to either human or animal use.

## 3 Results and discussion

Scheme 1 and Scheme 2 show the synthesis of PDCEA and PUDCEA. PDCEA, synthesized by chemical reaction (condensation) between HEJA and CDTA, was reacted with TDI through an addition reaction to form PUDCEA, which had added fumed silica (1wt%,2 wt%, and 3wt%). Beyond the 3wt% loading of fumed silica, the coating properties deteriorated. Acid values (20,15,13,12,10), hydroxyl values (261,60,58,57,55) and number of OH group per 100gm( 7.923,1.821,1.760,1.730,1.669) decreased from PDCEA toPUDCEA-3,with the descending order PDCEA>PUDCEA>PUDCEA-1>PUDCEA-2>PUDCEA-3. Refractive index values (1.4987, 1.5020, 1.5119, 1.5205, 1.5212) increased from PDCEA to PUDCEA-3.These values show noticeable increase, with an increased amount of fumed silica. The molecular weight of PUDCEA was found to be 6285(Mw) and 3928(Mw), with a polymer polydispersity index of 1.60 (Figure 1).The preparation of PDCEA and PUDCEA was confirmed by spectral analyses (FTIR and NMR). PUDCEA resins are soluble in xylene, toluene,



Scheme 1: Synthesis of PDCEA.



Scheme 2: Synthesis of PUDCEA.



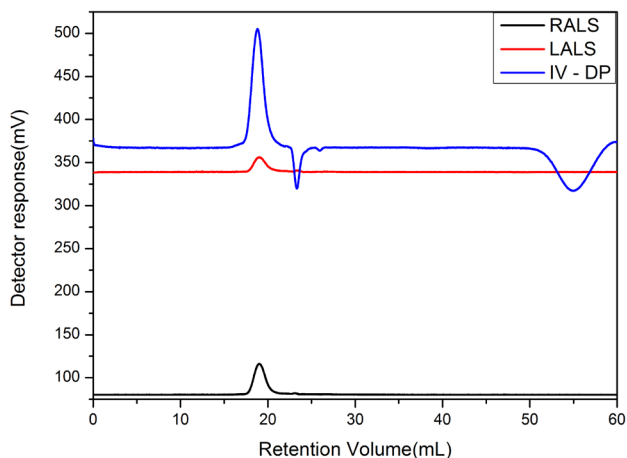


Figure 1: Chromatogram of PUDCEA.

dimethyl formamide (DMF), dimethyl sulphoxide (DMSO), chloroform and tetrahydrofuron (THF) and is soluble in aqueous solvent. The coated panels are left to dry at room temperature and the curing occurs in following steps: (i) the evaporation of solvent occurs, (ii) the free  $-NCO$  groups undergo curing at room temperature by reacting with atmospheric moisture, and (iii) the double bonds of fatty acid chain of oil also undergo auto-oxidation and the coating is finally cured over the substrate.

### 3.1 Spectral analysis

**PDCEA, FTIR ( $cm^{-1}$ ):** 3327(OH); 2925 ( $CH_2$ , asymmetrical); 2854 ( $CH_2$ , symmetrical); 1745 (C=O, ester); 1636(C=O, amide); 1454 (C-N, stretching); 3006 ( $-CH=CH-$ );

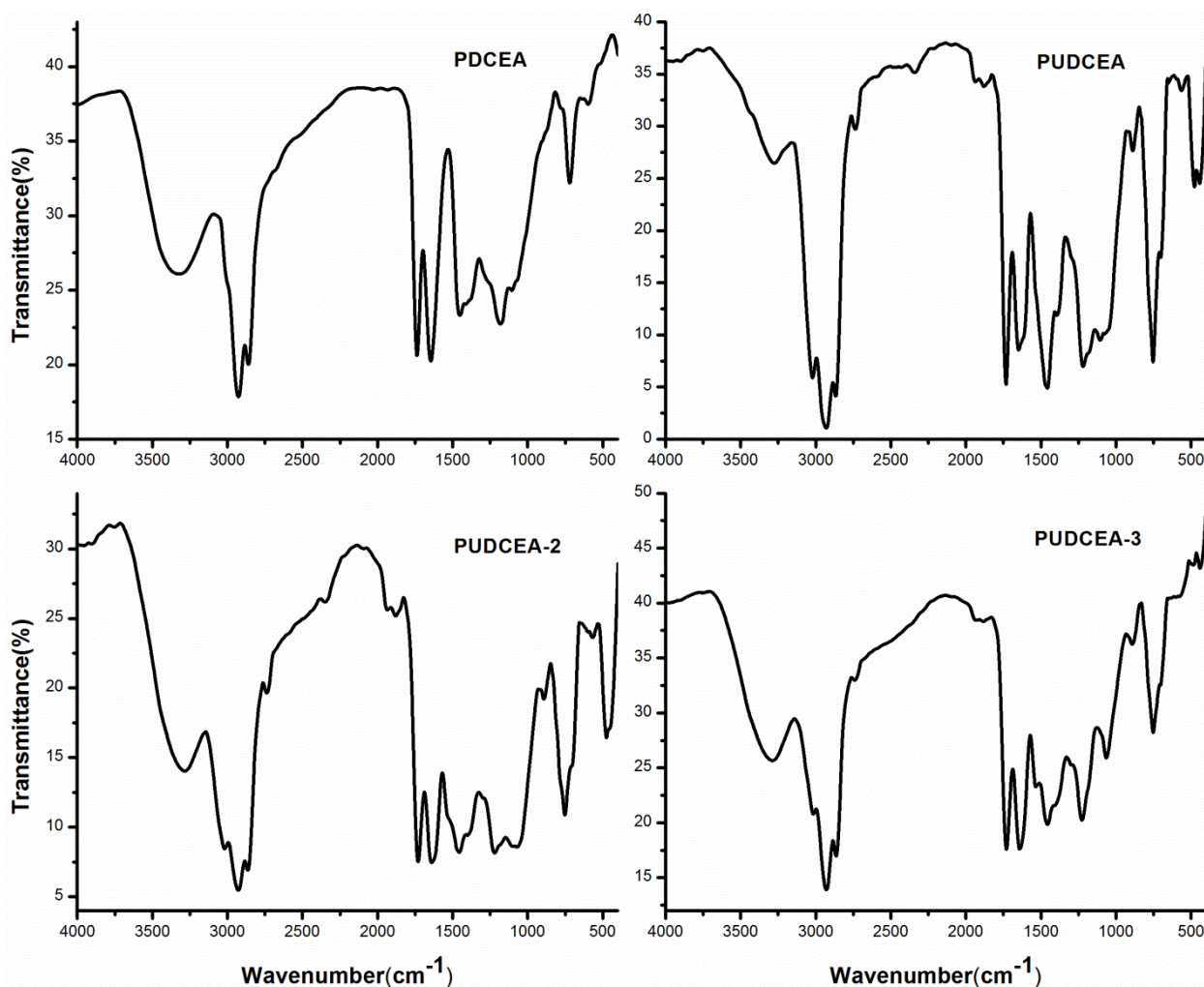


Figure 2: FTIR spectra of PDCEA, PUDCEA, PUDCEA-1 and PUDCEA-2.

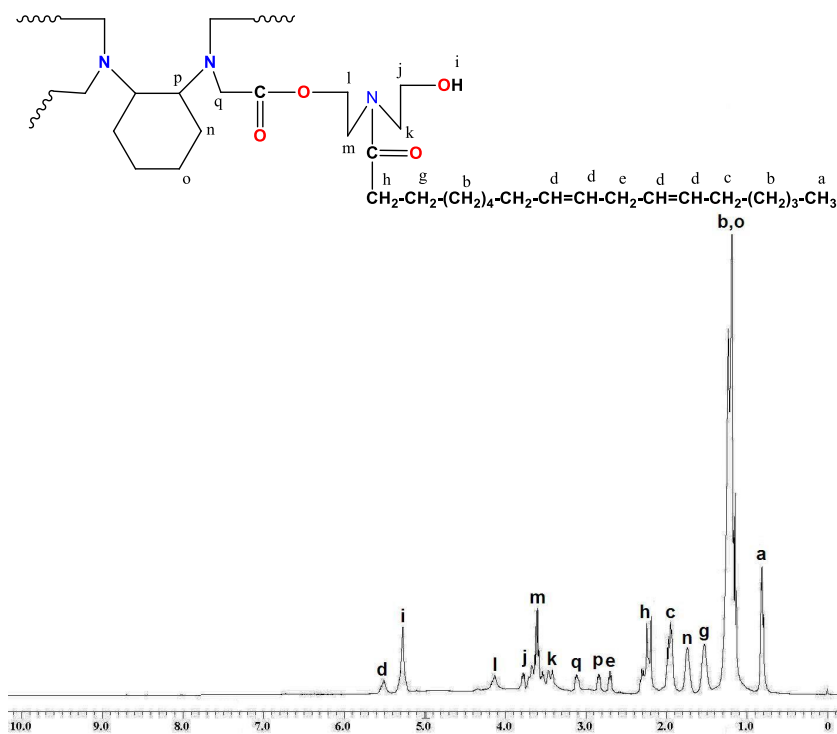


Figure 3:  $^1\text{H}$  NMR spectra of PDCEA.

1180,1090 ( $-\text{C}(\text{CO})\text{O}-\text{C}-$  stretching) (Figure 2). **PUDCEA:** 3300 (N-H, stretching); 3027 ( $-\text{CH}=\text{CH}-$ ); 2937( $\text{CH}_2$ , asymmetrical); 2846( $\text{CH}_2$ , symmetrical); 2719(C-H, stretching); 2337(free NCO); 1736(C=O, urethane, ester); 1646 (CO, amide); 1446 (C-N, stretching); 1227,1118,1046( $-\text{C}(\text{CO})\text{O}-\text{C}-$  stretching); 1500, 864,773 (aromatic); 700(NH, bending) (Figure 2). **PUDCEA-2** and **PUDCEA-3** showed additional bands at 1054 and 1064(O-Si-O) [31].

**PDCEA  $^1\text{H}$  NMR( $\text{CDCl}_3$ ,  $\delta$  ppm):** 0.846-0.892( $-\text{CH}_3$ ); 1.149-1.234( $-\text{CH}_2-$ , cyclic  $-\text{CH}_2-$ ); 1.590( $-\text{CO}-\text{CH}_2-\text{CH}_2-$ ); 1.751(cyclic  $-\text{CH}_2-$ ); 1.925( $-\text{CH}_2$  attached double bond); 2.242( $-\text{CH}_2$  attached CO); 2.732( $\text{CH}_2$  between double bond); 2.821(cyclic  $>\text{CH}-\text{N}<$ ); 3.151( $\text{CH}_2$  between CO and N); 3.480( $>\text{N}-\text{CH}_2-\text{CH}_2-\text{OH}$ ); 3.548(O- $\text{CH}_2-\text{CH}_2-\text{N}<$ ); 3.852( $>\text{N}-\text{CH}_2-\text{CH}_2-\text{OH}$ ); 4.143(O- $\text{CH}_2-\text{CH}_2-\text{N}<$ ); 5.252( $-\text{OH}$ ); 5.513( $\text{CH}=\text{CH}$ ) (Figure 3). Additional peaks for **PUDCEA:** 2.321( $\text{CH}_3$  of TDI); 7.012-7.350(aromatic proton); 7.850(NH, urethane) (Figure 4).

**PDCEA  $^{13}\text{C}$  NMR( $\text{CDCl}_3$ ,  $\delta$  ppm):** 13.995(terminal chain  $\text{CH}_3$ ); 22.064-26.690( $-\text{CH}_2-\text{CH}_3$ , cyclic  $-\text{CH}-$ ); 28.684( $-\text{CH}_2$  attached CO-); 30.092(chain  $-\text{CH}_2$ ); 31.512( $-\text{CH}_2$  attached double bond); 45.564( $-\text{CH}_2$  attached N); 50.051( $-\text{CH}_2-\text{CH}_2-\text{OH}$ ); 57.800( $-\text{CO}-\text{CH}_2-\text{N}<$ ); 60.021-66.231( $-\text{CH}_2\text{OH}$ ,  $-\text{CH}_2-\text{O}-$ , cyclic  $\text{CH}-\text{N}<$ ); 127.520-130.321( $-\text{CH}_2-\text{CH}=\text{CH}-$ ); 172.406-174.685(CO, amide, ester) (Figure 5). Additional peaks

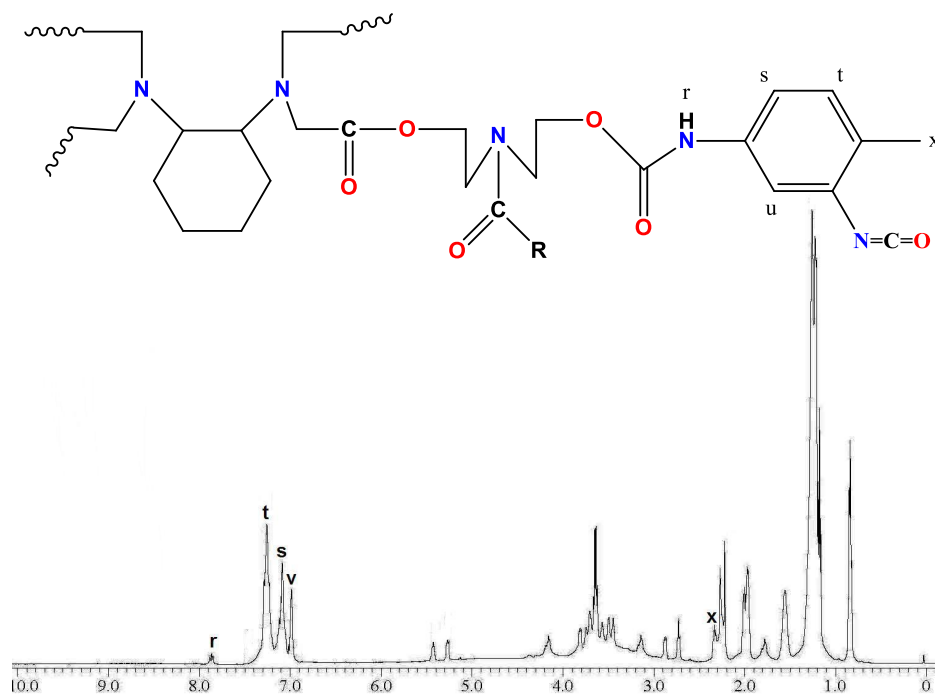
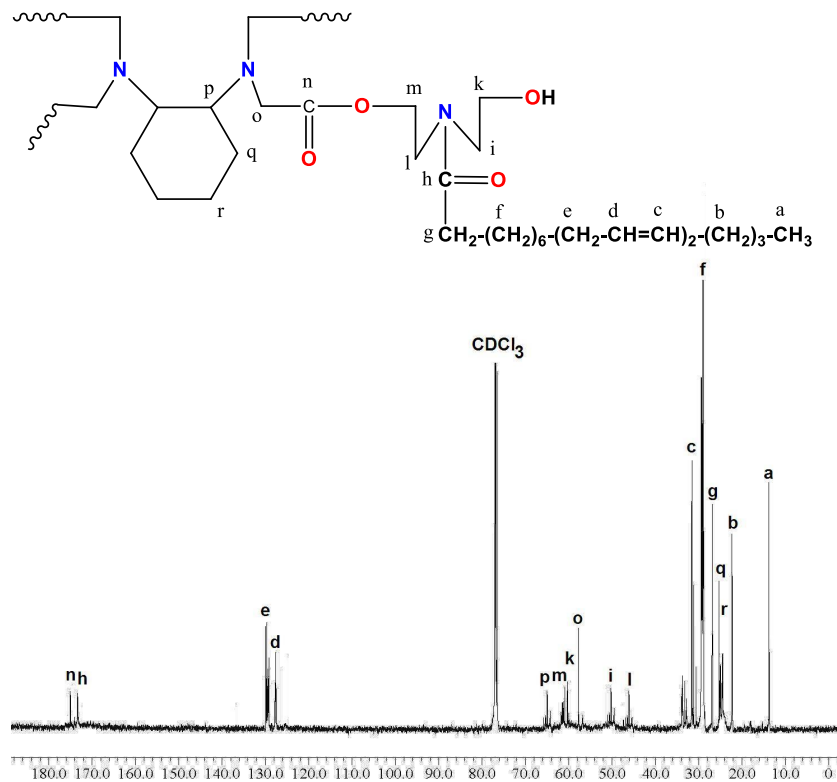
for **PUDCEA:** 19.021( $\text{CH}_3$  of TDI); 120.231-137.106(aromatic C); 144.213(free NCO); 165.021(CO, urethane) (Figure 6).

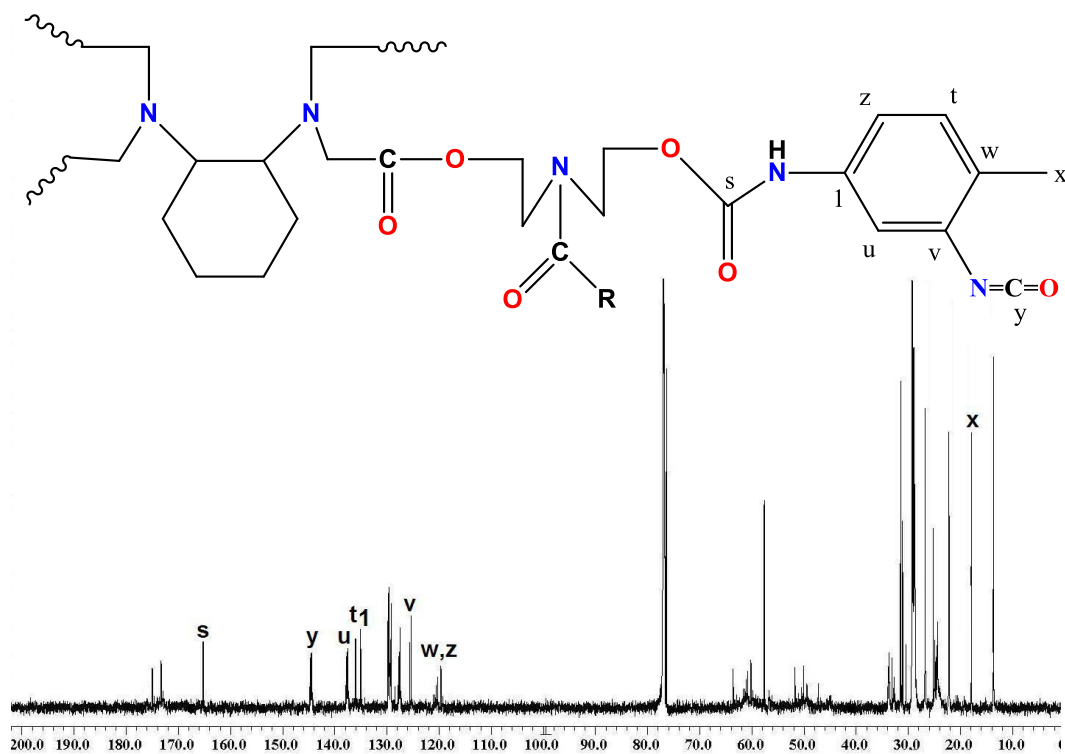
### 3.2 SEM and EDX analysis

SEM micrograph (Figure 7) of PUDCEA/fumed silica nanocomposite coating suggests that the coated film has uniform surface. There were no noticeable cracks; silica nanoparticles were not well-defined in shape, however, they showed an even dispersion in PUDCEA matrix. EDX spectrum supported the finding that  $\text{SiO}_2$  nanoparticles were present in PUDCEA matrix

### 3.3 Topography

Figure 7 show the topography of PUDCEA-2 nanocomposite coating before and after it was exposed to salt spray test. The initial topography of PUDCEA-2 (Figure 8A) reveals a smooth and uniform surface with nanoscale roughness (16 nm); the image distinctly reveals the even dispersion of silica nanoparticles in PUDCEA matrix. The AFM topography (Figure 8B) image after exposure in salt spray test indicates that coating surface has nanoscale

Figure 4:  $^1\text{H}$  NMR spectra of PUDCEA.Figure 5:  $^{13}\text{C}$  NMR spectra of PDCEA.

Figure 6:  $^{13}\text{C}$  NMR spectra of PUDCEA.

### JED-2200 Series

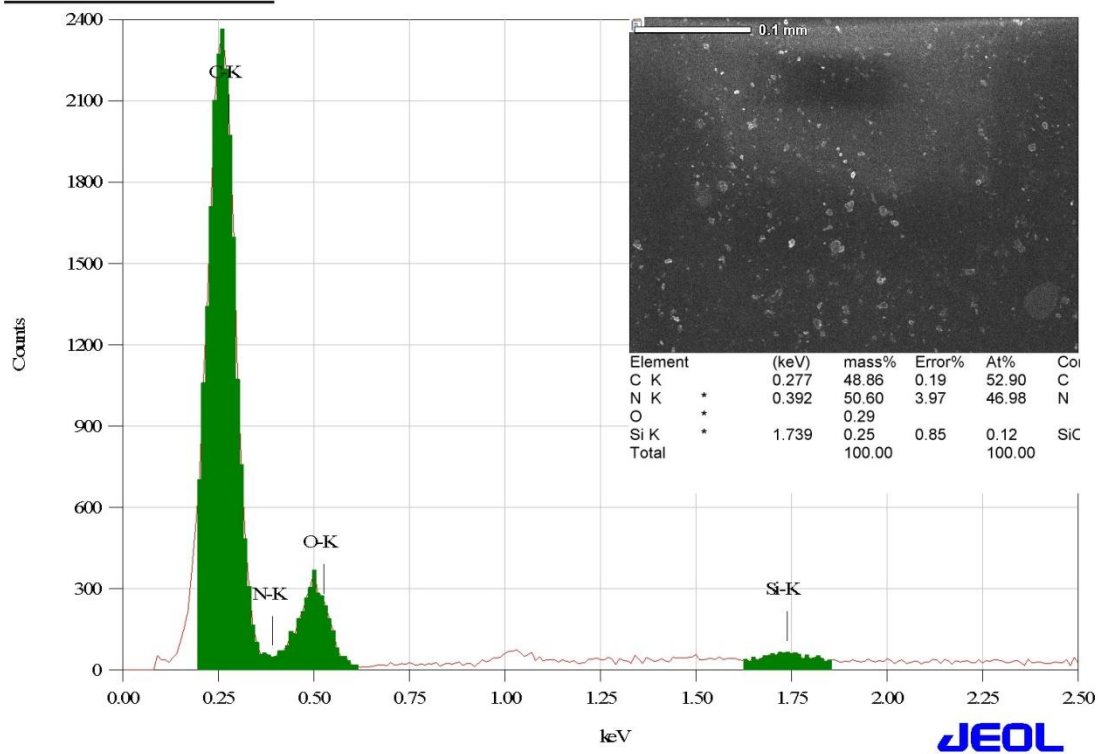
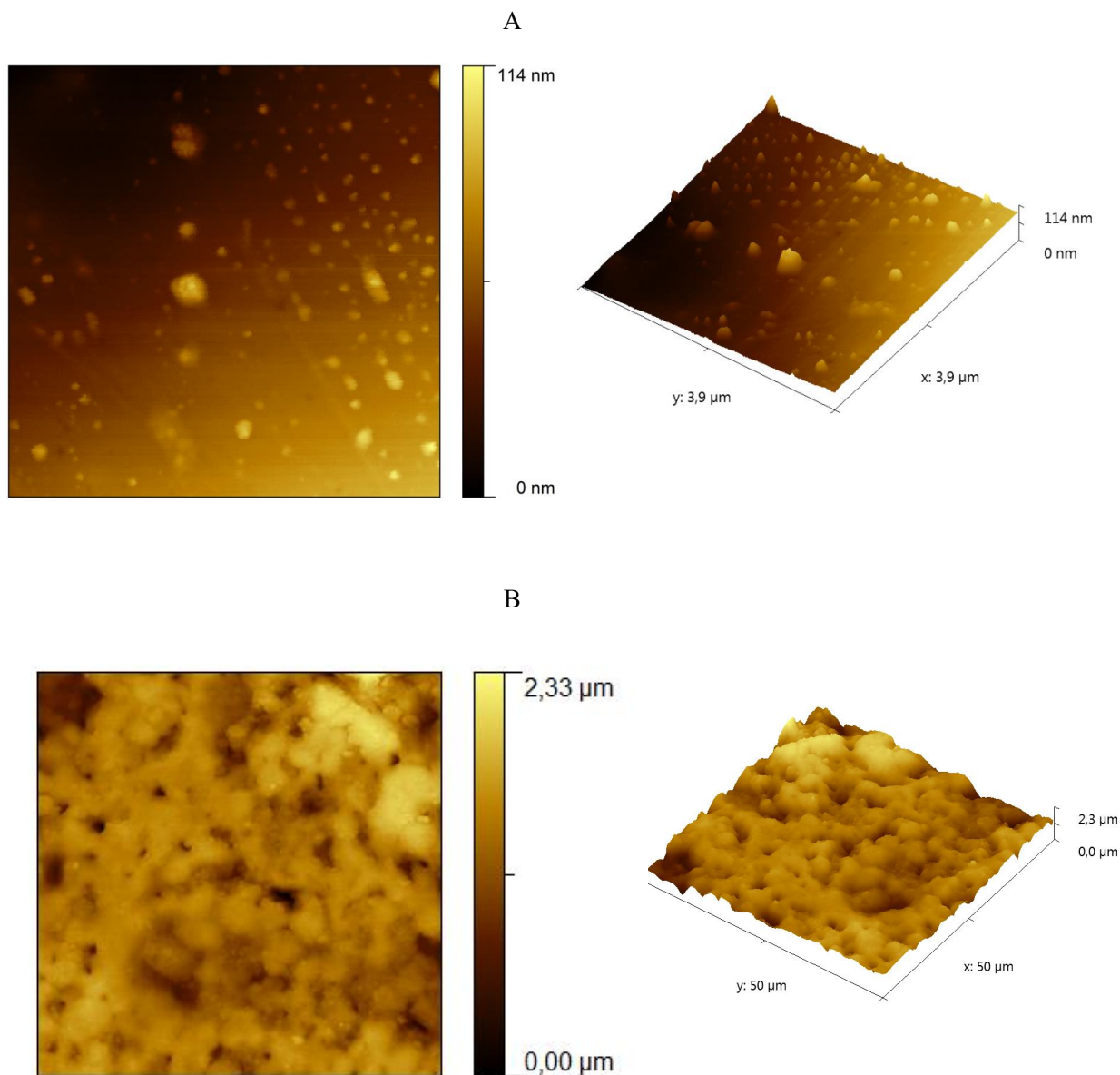


Figure 7: SEM-EDX of PUDCEA-2 nanocomposite.





**Figure 8:** (A) AFM topographic image of PUDCEA coating, (B) AFM topographic image of PUDCEA-3 coating surface after exposed in salt spray.

roughness (45 nm) and shows some defects in coating like pinholes, pores and increased surface roughness because solvent penetrated the coating surface.

### 3.4 Thermal analysis

Figure 9 shows TGA thermograms for PDCEA, PUDCEA, and PUDCEA-2 nanocomposite coatings. 5% weight loss of each sample at 257°C, 230°C and 245°C, respectively, can be correlated to the trapped solvent being evaporated. 50% weight losses of PDCEA, PUDCEA and PUDCEA-2 at 418°C,

424°C and 429°C are due to thermal degradation. DTG thermograms of PDCEA, PUDCEA and PUDCEA-2 clearly show each decomposition step in Figure 10. One peak in PDCEA runs between 288°C and 546°C, centered ( $T_{max}$ ) at 420°C. The peak in this particular temperature range corresponds to 50% weight loss in the TGA thermogram. In case of PUDCEA, three decomposition peaks are seen: one between 180°C and 305°C, centered ( $T_{max1}$ ) at 262°C; the second decomposition from 305°C to 440°C, centered ( $T_{max2}$ ) at 408°C; and the third decomposition from 440°C to 546°C, centered ( $T_{max3}$ ) at 480°C. In PUDCEA-2, the first decomposition begins at 176°C and ends at

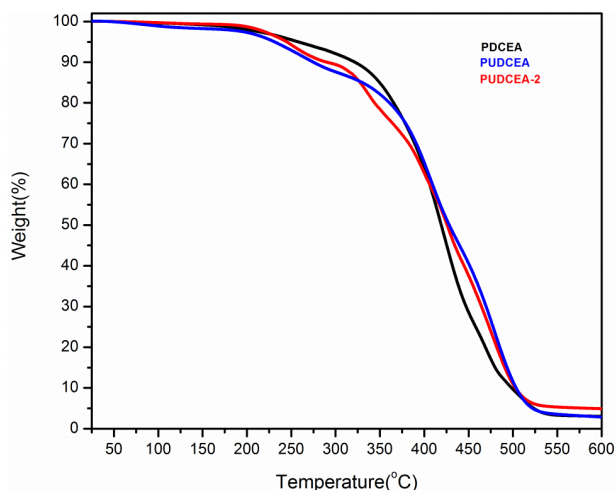


Figure 9: TGA thermogram of PDCEA, PUDCEA and PUDCEA-2.

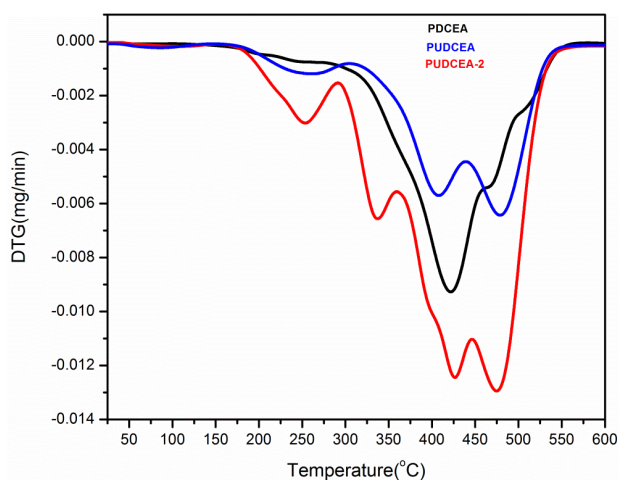


Figure 10: DTG thermogram of PDCEA, PUDCEA and PUDCEA-2.

210°C, centered ( $T_{max1}$ ) at 253°C; the second starts from 210°C to 360°C, centered ( $T_{max2}$ ) at 336°C; the third goes from 360°C to 446°C, centered ( $T_{max3}$ ) at 427°C; and a fourth decomposition starts at 446°C and ends at 546°C, centered ( $T_{max4}$ ) at 475°C. The first, second and third decomposition peaks of PUDCEA and PUDCEA-2 are due to the decomposition of urethane, ester and amide linkages, and hydrocarbon chains, respectively; slightly shifting of the peaks is due to the inclusion of nanoparticles and the formation of strong polymeric-inorganic interactions.

DSC thermograms (Figure 11) of PDCEA, PUDCEA and PUDCEA-2 show an endotherm peak observed to start at 125°C and end at 275°C, centered at 191°C; Second starts from 100°C to 313°C, centered at 215°C; and the third starts from 188°C and goes to 225°C, centered at 202°C,

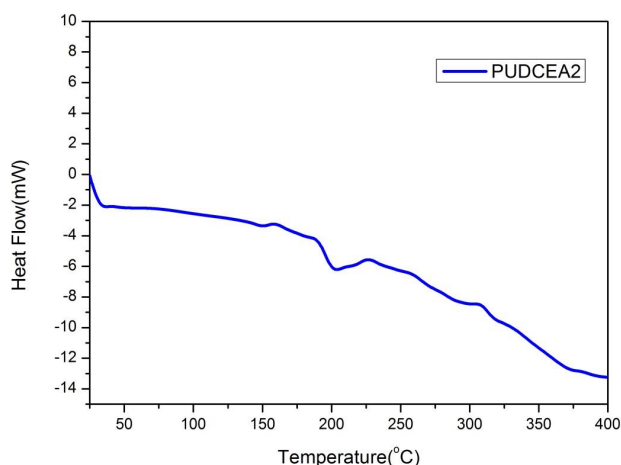
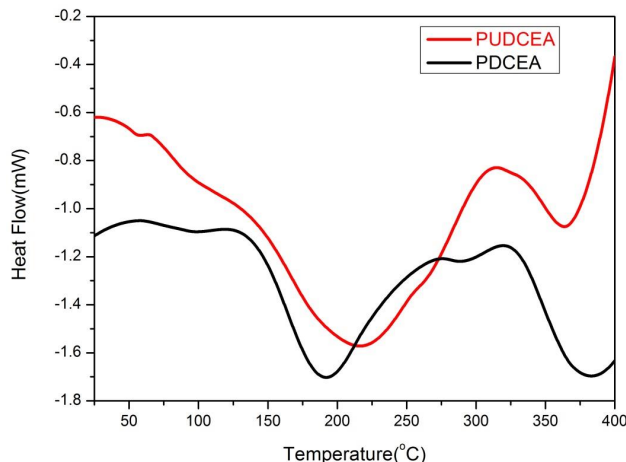
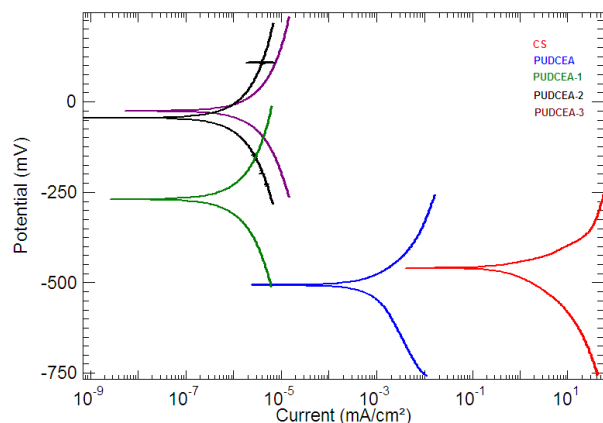


Figure 11: DSC thermogram of PDCEA, PUDCEA and PUDCEA-2.

respectively. These peaks can be attributed to the onset of melting of PDCEA, PUDCEA, and PUDCEA-2, followed by the decomposition process. An exotherm is seen beyond this temperature due to decomposition of resin as is also observed in TGA thermogram. Other small peaks are relevant to some configurational changes in the polymer chain backbone.

### 3.5 Physico-mechanical properties

PUDCEA coatings are produced by drying at ambient temperature. The coating thickness was obtained to be  $125 \pm 5 \mu\text{m}$ . The scratch hardness values of PUDCEA coatings increased from PUDCEA (1.8 kg) to PUDCEA-1 (2.5 kg), PUDCEA-2 (3.0 kg) and PUDCEA-3 (2.8 kg), beyond which the scratch hardness value deteriorated. The pencil hardness values were found to be 1B (PUDCEA), 2H (PUDCEA-1), 3H (PUDCEA-2), and HB (PUDCEA-3), deteriorating beyond PUDCEA-2. The coating properties deteriorate



**Figure 12:** Tafel plot of bare CS, PUDCEA, PUDCEA-1, PUDCEA-2 and PUDCEA-3 in HCl solution.

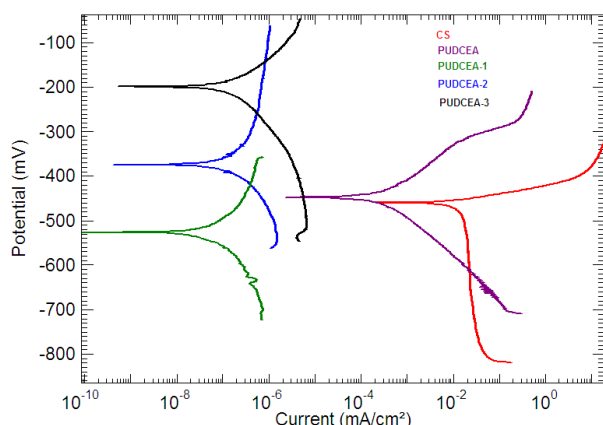


**Figure 13:** Tafel plot of bare CS, PUDCEA, PUDCEA-1, PUDCEA-2 and PUDCEA-3 in NaCl solution.

beyond 2wt% loading of fumed silica in PUDCEA resin. The coatings showed good impact resistance (150lb/inch), bending ability (1/8 inch) and the cross-hatch test results were 100%. The thickness of PUDCEA coating was approximately  $68 \pm 5 \mu\text{m}$ .

Beyond 3wt% loading, the performance of the coatings deteriorates. Silica particles increase the adhesion, flexibility and impact resistance of coatings due to good interactions between organic and inorganic phases. Beyond 3 wt% loading, there may be inadequate interactions between organic PU and inorganic Si phases, due to overloading of silica. The fumed silica particles occur as aggregates, these allow for particle-particle interactions and compactness in aggregates. We understand that 3wt% is the optimum loading of fumed silica for PU nanocomposites, and beyond 3wt% of fumed silica inclusion, the compactness between particles increases so much that it leads to rigidity, stiffness

and brittleness in coatings deteriorating the overall performance [36].

### 3.6 Corrosion studies

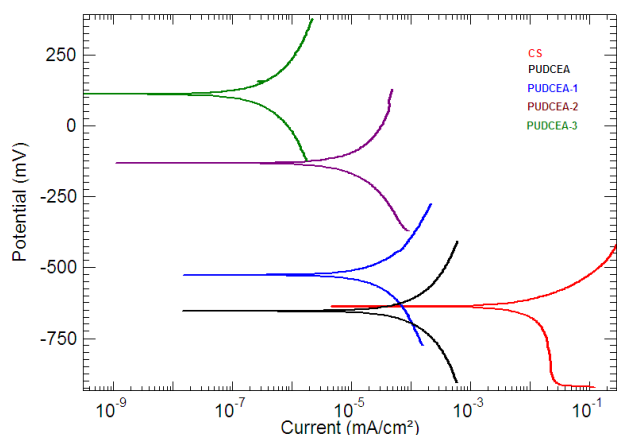
The Tafel plots (Figure 12) of bare carbon steel CS and PUDCEA, PUDCEA-1, PUDCEA-2, and PUDCEA-3 nanocomposite-coated CS permitted the determination of electrochemical parameters after immersion for 300h in an acidic medium. Table 1 summarizes the values of corrosion potential ( $E_{corr}$ ), corrosion current density ( $I_{corr}$ ), corrosion rates (CR) and linear polarization resistance ( $R_p$ ) of bare CS and PUDCEA, PUDCEA-1, PUDCEA-2, and PUDCEA-3 nanocomposite-coated CS. The polarization curve indicates positive displacement in  $E_{corr}$  relative the value of bare CS. The corrosion parameters for bare CS and PUDCEA coated CS clearly indicate that  $E_{corr}$ ,  $R_p$  increases from bare CS to PUDCEA, PUDCEA-1, PUDCEA-2 and PUDCEA-3, and  $I_{corr}$  values decreases. These observations indicate that PUDCEA provided a barrier method of corrosion protection for CS, thus enhancing the resistance towards corrosion. The corrosion potential shift indicates improved protection of CS by the barrier provided by PUDCEA coated on CS surface. PDP measurements clearly reveal reduction in CR for PUDCEA-3 coated surface ( $3.333E-06\text{mpy}$ ) with respect to the bare CS ( $25.049\text{mpy}$ ).

Figure 13 shows the Tafel plots after immersion for 240 h in a saline corrosive media.  $E_{corr}$  values of CS and PUDCEA, PUDCEA-1, PUDCEA-2, and PUDCEA-3 are given in Table 1. These values shifted to more positive values with increasing amounts of fumed silica in PUDCEA compared to bare CS.  $I_{corr}$  values decreased gradually and  $R_p$  values increased. The  $E_{corr}$ ,  $I_{corr}$ , and  $R_p$  values trends indicate the corrosion resistant nature of nanocomposite coating. PUDCEA coated CS with fumed silica nanoparticles show remarkable improvement in corrosion resistance properties. It is therefore likely that the presence of  $\text{SiO}_2$  particles in PUDCEA matrix provide protective barrier and reduce the interaction between  $\text{Cl}^-$  ions and the CS surface [37-38].

Figure 14 shows the Tafel plots of CS and PUDCEA, PUDCEA-1, PUDCEA-2 and PUDCEA-3 after an immersion period of 240h in tap water. As indicated in Table 1,  $E_{corr}$  values of PUDCEA coated panels showed an increase as the amount of fumed silica inclusion increased in coatings, and also higher values of  $R_p$  and smaller values of  $I_{corr}$  were observed relative to PUDCEA coated CS strips. The anticorrosive property of PUDCEA-3 film has been enhanced due to the dispersion of  $\text{SiO}_2$  in PUDCEA.

**Table 1:** Corrosion parameters for carbon steel (CS) and PUDCEA coated CS in various medium.

Code	$E_{cor}$ (mV)	$I_{cor}$ (mA/cm <sup>2</sup> )	Corrosion Rate(mm/year)	LPR (ohm.cm <sup>2</sup> )	Medium
CS	-459.29	2.1612	25.049	5.822	3.5wt% HCl
PUDCEA	-506.81	5.219E-04	6.052E-03	241.8	3.5wt% HCl
PUDCEA-1	-260.80	3.109E-07	8.603E-06	1.048E+07	3.5wt% HCl
PUDCEA-2	-32.902	3.316E-07	3.843E-06	3.795E+07	3.5wt% HCl
PUDCEA-3	-14.355	4.189E-07	3.333E-06	4.750E+07	3.5wt% HCl
CS	-568.78	0.475	1.022	96.505	3.5wt% NaCl
PUDCEA	-458.36	1.173E-03	1.360E-03	1072	3.5wt% NaCl
PUDCEA-1	-526.98	2.065E-07	5.334E-06	2.303E+08	3.5wt% NaCl
PUDCEA-2	-374.39	3.41E-07	4.589E-06	4.698+08	3.5wt% NaCl
PUDCEA-3	-197.43	4.339E-07	3.028E-06	4.559E+08	3.5wt% NaCl
CS	-671.03	4.693E-03	4.164E-02	16.356+05	Tap water
PUDCEA	-656.36	3.051E-05	3.837E-04	1.123E+05	Tap water
PUDCEA-1	-526.01	3.918E-06	1.034E-04	3.411E+06	Tap water
PUDCEA-2	-121.83	6.343E-06	3.875E-05	4.764E+06	Tap water
PUDCEA-3	126.97	1.003E-07	1.159E-06	1.258E-08	Tap water



**Figure 14:** Tafel plot of bare CS, PUDCEA, PUDCEA-1, and PUDCEA-2 and PUDCEA-3 in tap water.

The corrosion protection effect of PUDCEA-3 is attributed to an increase in amount of SiO<sub>2</sub> revealing a reduced permeability of coated surface to corrosive ions and diffusion pathways of water and oxygen, as compared to PUDCEA coating, due to presence of dispersed silica nanoparticles. It was found that lowest corrosion rates were exhibited under PUDCEA-3 nanocomposite film.

## 4 Conclusions

Poly(urethane esteramide) nanocomposites containing fumed silica were prepared from Jatropha oil, a sustainable resource. From this study, it can be concluded that sustainable Jatropha oil can be used successfully for the synthesis of PUDCEA-SiO<sub>2</sub> nanocomposite. PUDCEA-SiO<sub>2</sub> resins have good adhesion, hardness, gloss, and anticorrosive properties in various corrosive environments (tap water, 3.5wt% NaCl, and 3.5wt% HCl). PUDCEA-SiO<sub>2</sub> coating serves as a barrier to protect substrate, such as carbon steel surface. PUDCEA-fumed silica coatings can be used safely at temperatures up to 200°C.

**Acknowledgement:** The Project was supported by King Saud University, Deanship of Scientific Research, and College of Science - Research Center.

**Conflict of interest:** Authors declare no conflict of interest.



## References

- [1] Carisson A.S., Yilmaz J.L., Green A.G., Stymne S., Hofvander P., Replacing fossil oil with fresh oil- with what and for what?, *Eur. J. Lipid. Sci. Technol.*, 2011,113, 812- 831.
- [2] Sharmin E. Zafar F., Akram D., Alam M., Ahmad, S., Recent advances in vegetable oils based environment friendly coatings: A review. *Ind. Crops Prod.*, 2015, 76, 215-229.
- [3] Petrovic Z.S., Polyurethanes from vegetable oil, *Polymer Reviews*, 2008, 48, 109-155.
- [4] Alam M., Akram D., Sharmin E., Zafar F., Ahmad S., Vegetable oil based eco-friendly coating materials: A review article, *Arab. J. Chem.*, 2014, 7, 469-479.
- [5] Chen S., Wang Q., Wang T., X. Pei., Preparation, damping and thermal properties of potassium titanate whiskers filled castor oil- based polyurethane/epoxy interpenetrating polymer network composites, *Mater. Des.*, 2011, 32, 803-807.
- [6] Andrew J. C., Hoong S. S., Copolymers of tetrahydrofuran and epoxidized vegetable Oils: application to elastomeric polyurethanes, *Polym. Chem.*, 2014, 5, 3238-3244.
- [7] Dutta S., Karak N., Jana. T., Evaluation of mesua ferrea L. seed oil modified polyurethane paints. *Prog. Org. Coat.*, 2009, 65, 131-135.
- [8] Ferrer M.C.C., Babb D., A.J. Ryan., Characterisation of polyurethane networks based on vegetable derived polyol, *Polymer*, 2008, 49, 3279-3287.
- [9] Koprululu A., Onen A., Serhatli I.E., Guner F.S., Synthesis of triglycerides-based urethane macromers and their use in copolymerization, *Prog. Org. Coat.*, 2008, 63, 365-371.
- [10] Chaudhari A., Kulkarni R., Mahulikar P., Sohn, D., Gite V., Development of PU coatings from neem oil based alkyds prepared by the monoglyceride route, *J. Am. Oil Chem. Soc.*, 2015, 92, 733-741.
- [11] El-Wahab H. A., EL-Fattah M. A., Ghazy M.B.M. Synthesis and characterization of new modified anti-corrosive polyesteramide resins incorporated pyromellitimide ring for surface coating, *Prog. Org. Coat.*, 2011, 72, 353-359.
- [12] Meshram P. D., Puri R. G. Patil A. L., Gite V.V., Synthesis and characterization of modified cottonseed oil based polyesteramide for coating applications, *Prog. Org. Coat.*, 2013, 76, 1144-1150.
- [13] Lligadas G., Ronda J. C., Galia M., Biermann U., Metzger J.O., Synthesis and characterization of polyurethanes from epoxidized methyl oleate based polyether polyols as renewable resources, *J. Polym. Sci. Part A Polym. Chem.*, 2006, 44, 634-645.
- [14] Alam M., Alandis N. M., Microwave-assisted preparation of urethane-modified polyetheramide coatings from jatropa seed oil, *High Perform. Polym.*, 2012, 24(6), 538-545.
- [15] Alam M., Alandis, N. M., Microwave assisted synthesis of urethane modified polyesteramide coatings from jatropa seed oil, *J. Polym. Environ.*, 2011, 19, 784-792.
- [16] Hubicka H., Kolodynska D., Separation of rare-earth element complexes withtrans-1,2-diaminocyclohexane-N,N,NV-tetraacetic acid on polyacrylate anion exchangers, *Hydrometallurgy*, 2004, 71, 343-350.
- [17] Martim-Ramos J.D., Tercero-Moreno J.M., Matilla-Hernandez A., Niclos-Gutierrez J., Busnot, A., Copper(II) and nickel(II) chelates with dihydrogen trans1,2 diaminocyclo-hexane-N,N,N',N',-tetraacetate<sup>(2-)</sup> ion(H<sub>2</sub>CDTA<sup>2-</sup>). Synthesis, XRD structure and properties of [Cu(H<sub>2</sub>CDTA)].H<sub>2</sub>O and [Ni(H<sub>2</sub>CDTA).H<sub>2</sub>O].4H<sub>2</sub>O, *Polyhedron*, 1996, 15, 439-496.
- [18] Dybczynski R., Wodkiewicz L., Effect of temperature on anion exchange of the rare earthtrans1,2diaminocyclo-hexane-N,N',-tetraacetates and the structure of complex ions, *J. Inorg. Nucl. Chem.*, 1969, 31, 1495-1506.
- [19] Hecht M., Fawcett W.R., An electrochemical study of solvent-complex interaction in trans1,2 diaminocyclo-hexane-N,N,N',N',-tetraacetatochromate(III) and 1,2 diaminoethane-N-hydroxyethyl-N, N',N'- tri acetatochromium(III), *Electrochimica Acta*, 1996, 41, 1423-1433.
- [20] Montazeri A., Khavandi A., Javadpour J., Tcharkhtchi A., The Effect of Curing Cycle on the Mechanical Properties of MWNT/ Epoxy Nanocomposite, *Int. J. Polym. Anal. Charact.*, 2010, 15(3), 182-190.
- [21] Alam M., Sharmin E., Alandis N. M., Ahmad. N., Effect of organoclay on structure, morphology, thermal behavior and coating performance of jatropa oil based polyesteramide, *e-Polymers*. 2017, 17(6), 491-500.
- [22] Rahman O., Kashif M., Ahmad. S., Nanoferrite dispersed waterborne epoxy-acrylate: anticorrosive nanocomposite coatings, *Prog. Org. Coat.*, 2015, 80, 77-86.
- [23] Sung L.P., Comer J., Forster A. M., Hu H. Floryancic B. Brickweg L., Fernando, R.H., Scratch behavior of nano-alumina/ polyurethane coatings, *J. Coat. Technol. Res.*, 2008, 5, 419-430.
- [24] Sangermano M., Malucelli G., Amerio E., Priola A., Billi E., Rizza G., Photopolymerization of epoxy coatings containing silica nanoparticles, *Prog. Org. Coat.*, 2005, 54, 134-138.
- [25] Cui C., Ding H., Cao L., Chen, D., Preparation of CaCO<sub>3</sub>-SiO<sub>2</sub> composite with core-shell structure and its application in silicone rubber, *Pol. J. Chem. Tech.*, 2015, 17(4), 128-133.
- [26] Shi H., Liu F., Yang L., Han. E., Characterization of protective performance of epoxy reinforced with nanometer-sized TiO<sub>2</sub> and SiO<sub>2</sub>, *Prog. Org. Coat.*, 2008, 62, 359-368.
- [27] Osvath Z., Toth T., Ivan B., Synthesis, characterization, LCST-type behavior and unprecedented heating-cooling hysteresis of poly(N-isopropylacrylamide-co-3(trimethoxysilyl)propyl methacrylate) copolymers, *Polymer*, 2017,108, 395-399.
- [28] Osvath Z., Toth T., Ivan B., Sustained drug release by thermoresponsive sol-gel hybrid hydrogels of poly(N-isopropylacrylamide-co-3(trimethoxysilyl)propyl methacrylate) copolymers. *Macromol. Rapid Commun*. 2017, 38(6), 1600724, DOI: 10.1002/marc.201600724
- [29] Zhong J., Lin G., Wen W.Y., Jones A. A., Kelman S., Freeman B. D., Translation and rotation of penetrants in ultra permeable nanocomposite membrane of poly(2,2-bis(trifluoromethyl)-4,5-difluoro-1,3-dioxole-co-tetrafluoroethylene)and fumed silica, *Macromolecules*, 2005, 38(9), 3754-3764.
- [30] Yeh J.M., Chang K.C., Polymer/layered silicate nanocomposite anticorrosive coatings, *J. Ind. Eng. Chem.*, 2008, 14, 275-291.
- [31] Wu G., He X., Xu L., Zhang H., Yan. Y., Synthesis and characterization of bio based polyurethane/SiO<sub>2</sub> nanocomposites from natural Sapium sebiferum oil, *RSC Adv*, 2015, 5, 27097.
- [32] Czech Z. Maciejewski Z., Kondratowicz-Maciejewska K., Waterborne pressure-sensitive adhesives acrylics modified using amorphous silica nanoparticles *Pol. J. Chem. Tech.*, 2016, 18(4), 124-128.



- [33] Protsaka I., Tertykha V., Pakhlova E., Derylo-Marczewskaca A., Modification of fumed silica surface with mixtures of polyorganosiloxanes and dialkyl carbonates, *Prog. Org. Coat.*, 2017, 106, 163-169.
- [34] Alam M., Alandis N. M., Ahmad N., Development of poly(urethane-ester)amide from corn oil and their anticorrosive studies, *Int. J. Polym. Anal. Charact.*, 2017, 22(4), 281-293.
- [35] Sari M.G., Ramezanzadeh B., Shahbazi M., Pakdel A.S., Influence of nanoclay particles modification by polyesteramide hyperbranched polymer on the corrosion protective performance of the epoxy nanocomposite, *Corros Sci.*, 2017, 92, 162-72.
- [36] Akram D., Sharmin E., Ahmad S. Linseed polyurethane/ tetraethoxyorthosilane/fumed silica hybrid nanocomposite coatings: Physico-mechanical and potentiodynamic polarization measurements studies. *Prog. Org. Coat.*, 2014, 77(5), 957-964.
- [37] Pirvu C., Demetrescu I., Drob P., Vasilescu E., Vasilescu C., Mindroiu M. & Stancuc R., Electrochemical stability and surface analysis of a new alkyd paint with low content of volatile organic compounds, *Prog. Org. Coat.*, 2010, 68, 274-82.
- [38] Li F., Li G., Zeng J., Gao G.H., Molybdate-doped copolymer coating for corrosion prevention of stainless steel, *J. Appl. Polym. Sci.*, 2014, 131, 40602–40609.